Audio Engineering Society
Convention Paper
Presented at the 133rd Convention
2012 October 26–29 San Francisco, CA, USA

Low-frequency temporal accuracy of small-room sound reproduction

Adam J. Hill[1] and Malcolm O.J. Hawksford[2]

[1] School of Technology, University of Derby, Derby DE22 3AW, UK
a.hill@derby.ac.uk

[2] School of Computer Science and Electronic Engineering, University of Essex, Colchester CO4 3SQ, UK
mjh@essex.ac.uk

ABSTRACT

Small-room sound reproduction is strongly affected by room-modes in the low-frequency band. While the spectral impact of room-modes is well understood, there is less information on how modes degrade the spatiotemporal response of a sound reproduction system. This topic is investigated using a bespoke finite-difference time-domain (FDTD) simulation toolbox to virtually test common subwoofer configurations using tone bursts to judge waveform fidelity over a wide listening area. Temporal accuracy is compared to the steady-state frequency response to determine any link between the two domains. The simulated results are compared to practical measurements for validation.

1. INTRODUCTION

Small-room acoustics has been a well-researched area for many years now. A significant volume of published work focuses on the acoustical characteristics of the low-frequency band in these spaces, emphasizing the detrimental effects of room-modes on the sound energy distribution over a wide listening area.

Room-modes are a result of standing waves between two or more surfaces which give rise to highly position-sensitive low-frequency responses. There is a wealth of methodologies geared towards reducing sound pressure spatial variance including: room dimension optimization [1,2], single or multiple subwoofer placement [3,4], passive or active absorption [5-7], single or multiple point equalization (either static or adaptive) [8-12] and subwoofer polar pattern control [13,14], among other varieties of correction [15,16].

Although many room-mode correction methods utilize a complex frequency response, most demonstrate correction performance in terms of the resulting magnitude response, often with the assumption that the phase response experiences similar improvements. While this assumption *may* be valid if room responses are minimum phase (where the magnitude and phase responses are directly related by the Hilbert transform [17]), it is less clear how the two are related when the complex frequency response contains non-minimum phase components and, even with a minimum phase relationship, whether the magnitude and phase errors always are strongly correlated.

This work takes the initial stance that there is no guaranteed relationship between low-frequency magnitude and phase error in small-room applications. The subsequent investigation examines the magnitude and phase errors side-by-side to determine their correlation and to formulate an explanation for any disparities. The highlighted incongruities emphasize the importance of ensuring low phase error alongside magnitude response homogeneity; a critical requirement of any high-quality sound reproduction system.

Section 2 of this paper reviews low-frequency room acoustics, measurement techniques and quantification of response error (including references for further study). Readers may skip to section 3 if a review of these subjects is not necessary.

2. LOW-FREQUENCY ROOM ACOUSTICS

The range defined as the low-frequency band in acoustics is dependent on the acoustical topology of a closed space. The most common measure for the upper limit of this band is the Schroeder frequency, f_s, which is calculated using Eq. 2.1, where RT_{60} is the reverberation time (s) and V is the room volume (m^3). A derivation of the constant in Eq. 2.1 is given in [18].

$$f_s = 2000\sqrt{\frac{RT_{60}}{V}} \tag{2.1}$$

As an example, a 5 m x 4 m x 3 m (120 m^3 volume) room with an average reverberation time of 200 ms has a Schroeder frequency of 115 Hz, indicating that the low-frequency range falls below this point. In this range, all room-modes are spatially and spectrally discrete and are therefore individually perceptible by humans. Room-modes also exist in the higher frequency range, however there is significant modal overlap which suppresses the ability to discern discrete modes [19].

Specific modal frequencies, f_m, are calculated for closed rectangular spaces using Eq. 2.2 [14,18] which is based on the rectangular dimensions (l_x, l_y, l_z) in meters, the modal indices (η_x, η_y, η_z), which correspond to how many half-wavelengths can fit within each dimension, and the speed of sound in air, c (m/s).

$$f_m = \frac{c}{2}\sqrt{\left(\frac{\eta_x}{l_x}\right)^2 + \left(\frac{\eta_y}{l_y}\right)^2 + \left(\frac{\eta_z}{l_z}\right)^2} \tag{2.2}$$

Although room-modes are present in any closed-space, it is difficult to calculate modal frequencies for non-rectangular spaces using a closed-form solution. This work deals with rectangular topologies, therefore the predictions from Eq. 2.2 are acceptable moving forward.

An in-depth discussion on the finer points of low-frequency room acoustics is presented in [14].

2.1. Measurement techniques

A number of measurement techniques exist which allow for a detailed examination of a room's acoustical characteristics. There are, of course, advantages and disadvantages to each approach. Two of these approaches are discussed here.

A maximum length sequence (MLS) is well-suited for objective acoustical measurements in a noisy environment. As an MLS is a pseudo-random binary signal consisting of a repeatable pattern, an impulse response can be extracted by determining the correlation of the input MLS to the measured signal. MLS tests have been known to exhibit certain amounts of harmonic distortion which can be avoided by generating multiple MLS signals of the same order, but with different recursion relations, and then averaging the resulting impulse responses [20].

While MLS testing allows for close inspection of the complex frequency response, it does not necessarily relate well to the subjective impression of a space. If human perception is of interest, a number of researchers recommend tone bursts. The tone burst is not new and has been used extensively since the 1950s for non-anechoic loudspeaker measurements [21-23].

An even symmetric tone burst is generated by windowing a sinusoid. The window can be any shape, but a raised cosine is commonly used [24] with the bandwidth of the signal related to the length of each burst in cycles. The shorter the window the higher the bandwidth, which is demonstrated in the limit by letting the burst duration tend to zero. In this case the burst has become a Dirac delta function, covering the entire bandwidth (at least up to the Nyquist frequency if the data is digitally sampled). On the contrary, if the burst was stretched to an infinite duration then the bandwidth collapses to a single frequency (pure tone). This is analogous to the uncertainty principle in quantum mechanics, where this case deals with Fourier analysis.

Following the work of Linkwitz [24,25], it has become common to use tone bursts for subjective evaluation. Linkwitz argues that when used appropriately, tone bursts bring out the spectral and temporal problems of a space. He suggests that a 10-cycle burst (roughly corresponding to a 1/3 octave bandwidth) repeated four times (allowing for the room to reach steady-state so that magnitude response can be inferred from the measured burst amplitude) relates closely to what is heard during normal program material playback.

An advantage to tone burst testing is that both magnitude and phase error can be judged instantly, albeit only one narrow-band at a time. This is achieved by oscilloscope measurement or by ear, an option not provided in MLS or similar measurements. Locating the "sweet-spot" is simply a matter of walking about to find a position with the best temporal and spectral accuracy. Of course this can be tedious if analysis is required over a wide bandwidth. If subjective testing is not required, data achieved with tone burst testing can be extracted from an impulse response calculated from MLS (or similar measurement) data.

2.2. Quantification of error

Objective analysis of measurement data often requires a set of metrics to best analyze the findings. In terms of low-frequency acoustics, there exists a small set of useful room response quality quantifiers including: spatial variance, magnitude deviation and mean absolute error. Each of these metrics is discussed herein.

Spatial variance is the measure of how much, on average, the frequency response deviates from point-to-point in a listening area (quantified in decibels). A low spatial variance implies superb frequency response homogeneity between listeners, while a high spatial variance indicates poor response correlation between listeners. Spatial variance (SV) is calculated with Eq. 2.3 where N_f is the number of frequency bins, f_{lo} and f_{hi} define the frequency range (Hz), N_p is the number of measurement points, $L_p(p, i)$ is the sound pressure level at point p in the i^{th} frequency bin, and $\overline{L_p(i)}$ is the mean sound pressure level across all measurement points in the i^{th} frequency bin [14].

$$SV = \frac{1}{N_f} \sum_{i=f_{lo}}^{f_{hi}} \sqrt{\frac{1}{N_p - 1} \sum_{p=1}^{N_p} \left(L_p(p,i) - \overline{L_p(i)}\right)^2} \tag{2.3}$$

While spatial variance is a metric for the overall sound energy distribution across a listening area, there may be instances when a point-by-point analysis is required. Magnitude deviation allows for such an analysis as it quantifies how much the frequency response varies from the room average response at a specified point (also quantified in decibels). Magnitude deviation (MD) is calculated using Eq. 2.4 where all variables are identical to Eq. 2.2 except without a sweep over measurement points as this metric focuses on one point at a time [14].

$$MD = \sqrt{\frac{1}{N_f - 1} \sum_{i=f_{lo}}^{f_{hi}} \left(L_p(p,i) - \overline{L_p(i)}\right)^2} \tag{2.4}$$

Spatial variance and MD deal with the steady-state response of a room. Both are very useful for quantifying low-frequency acoustical problems in a space, but they do not tell the entire story. An additional metric is needed to quantify the temporal behavior of a sound field. Mean absolute error (MAE) is one such metric used for this purpose. MAE is a measure of disagreement between two signals. For acoustical measurements this can be the difference between the source and measured signals. MAE is calculated with Eq. 2.5 where N is the total number of samples and s_i and y_i are the i^{th} samples from the source and measured signals, respectively.

$$MAE = \frac{1}{N} \sum_{i=1}^{N} \left| s_i - y_i \right| \tag{2.5}$$

In some cases it may be more beneficial to compare the energy envelopes of the signals (such as with tone bursts). This is achieved by applying a Hilbert transform to the source and measured signals as highlighted in the forthcoming sections.

3. MAGNITUDE AND PHASE ERROR AGGREEMENT

The relationship between magnitude and phase error is crucial to understanding the correction of room-modes. The underlying question is whether magnitude and phase response error over a listening area are always strongly correlated. Could it be that a perfectly corrected magnitude response (minimal spatial variance) does *not* result in correspondingly high waveform fidelity (minimal phase error)? This is an issue that is rarely investigated when describing modal correction methods, where it is often assumed that phase error is corrected along with magnitude error.

3.1. Impulse response data extraction

Before proceeding to error measurement and analysis, it is worth confirming that the temporal data acquired using tone bursts can alternatively be acquired from an impulse response. As long as all data of interest can be extracted from a set of impulse responses, the work can move forward with confidence of data accuracy.

A rectangular room of dimensions 5 m x 4 m x 3 m was modeled using a finite-difference time-domain algorithm [14]. An omnidirectional subwoofer was placed at a room corner (0.4 m, 0.4 m, 0.4 m) and a single measurement point was located at (3.0 m, 2.0 m, 1.8 m). All surfaces were set to 10% frequency-independent absorption.

Two signals were investigated: a 13th order MLS and an 80 Hz tone burst (10 cycles per burst, 4 repetitions). An impulse response was calculated from the MLS data and convolved with the source tone burst signal. The direct tone burst measurement was compared to the impulse response-derived tone burst measurement by calculating the error between the two signals (Fig. 3.1).

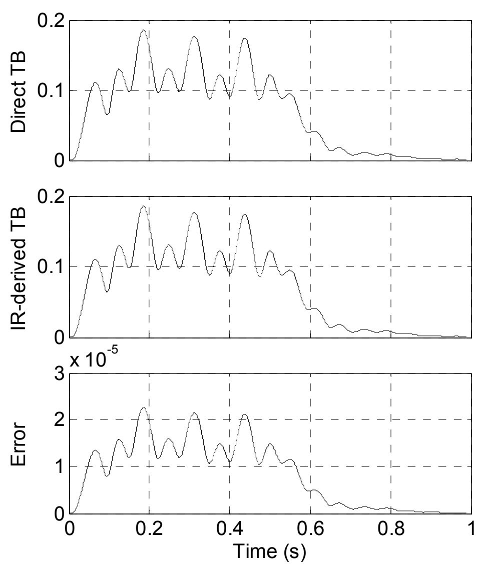

Fig. 3.1 80 Hz tone burst measurements (amplitude envelopes) for (top) direct measurement, (middle) impulse response-derived tone burst where (bottom) is the error between the top two data sets

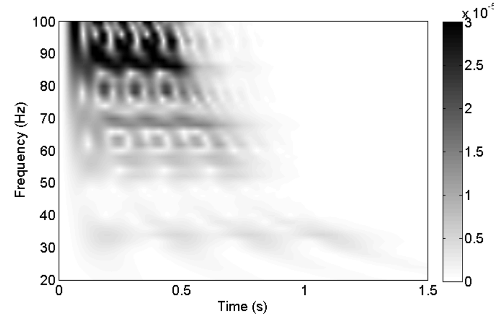

Fig. 3.2 Absolute error between direct and impulse response-derived tone burst measurements

The error between the direct and impulse response-derived tone bursts is negligible and follows the tone burst amplitude envelope precisely. The slight disagreement is likely due to rounding errors in the impulse response to tone burst derivation. A similar procedure was carried out over the entire low-frequency band (taken as 20 – 100 Hz in this case) with results presented in Fig. 3.2, showing that error increases with frequency, but nonetheless remains negligible.

3.2. Phase response analysis

As many room-mode correction procedures are presented with only magnitude response correction results, it is worthwhile to investigate the impulse response data for any excess phase components. An ideal electroacoustic sound reproduction system should be minimum phase, although this is rarely achieved due to room acoustics. At low-frequencies, however, the system may still exhibit minimum phase behavior, although measurements will contain a linear phase component due to the source to receiver propagation delay. The linear phase contribution for a frequency, *f*, is related to the propagation delay, τ_{prop}, by Eq. 3.1.

$$\phi_{linear} = -2\pi f \tau_{prop} \tag{3.1}$$

The ideal phase response can be calculated from the magnitude response, $|H(j\omega)|$, generated using the Fourier transform of the measured impulse response. This is achieved by taking the Hilbert transform (denoted as the operator H^T, not to be confused with the complex frequency response, $H(j\omega)$) of the magnitude response (Eq. 3.2). The measured phase response is determined from the complex frequency response and subtracting the linear phase component due to the propagation delay (Eq. 3.3). The measured phase response should highlight any excess phase components that aren't detected using the ideal phase calculation from the magnitude response.

$$\phi_{ideal} = -\mathrm{H}^T \left(\log\left|H(j\omega)\right|\right) \tag{3.2}$$

$$\phi_{meas} = \tan^{-1}\left(\frac{\mathrm{Im}\left(H(j\omega)\right)}{\mathrm{Re}\left(H(j\omega)\right)}\right) - \phi_{linear} \tag{3.3}$$

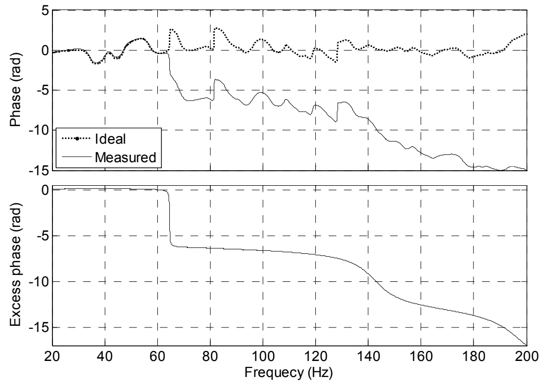

Fig. 3.3 Comparison of ideal and measured phase responses (top) and the excess phase components of the measured phase response (bottom)

This procedure was applied to the simulation data under inspection from 20 – 200 Hz. The ideal and measured responses were directly compared, where the excess phase components are highlighted (Fig. 3.3).

Below around 120 Hz the system exhibits minimum phase behavior, therefore (at least in this case) it is valid to inspect the magnitude response assuming the phase response is directly related. The only anomaly highlighted in this analysis is the sharp drop around 64 Hz. This is a result of the phase unwrapping procedure and has nothing to do with the system in question. After the jump, the excess phase remains at -2π until the system begins to display certain non-minimum phase characteristics around 120 Hz.

Interestingly, this roughly corresponds to the space's Schroeder frequency (~115 Hz), possibly indicating that the discrete modal region can be defined as the low-frequency band exhibiting minimum phase behavior. This point is not explored beyond this general statement, but would be an interesting topic for further investigation.

As the excess phase component analysis gives little information regarding phase response errors in the low-frequency band, it may be beneficial to inspect the level of phase response variance over narrow frequency bands. Since tone burst signals have a finite bandwidth (and relate very closely to real-world program material [25]), the variance between phase components over the bandwidth of a particular tone burst should indicate the level of coherency of the waveform as it arrives at the measurement location. High variance levels indicate the frequency components of the burst do not arrive simultaneously, causing a poor transient response.

Phase variance, *PV(f)*, for center frequency, *f*, is calculated as the difference between the ideal phase response ($\phi_{ideal}(i)$) at the i^{th} frequency bin and the mean ideal phase response ($\overline{\phi_{ideal}}$) over the entire analysis frequency range which is defined by the number of cycles per tone burst, N_c, and consists of N_f frequency bins (Eq. 3.4).

$$PV(f) = \frac{1}{N_f - 1} \sum_{i=f-f/N_c}^{f+f/N_c} \left(\phi_{ideal}(i) - \overline{\phi_{ideal}}\right)^2 \tag{3.4}$$

An example of this form of analysis is given in Fig. 3.4 using the setup from the previous example. Variance from the ideal phase progression was computed for 10-cycle tone bursts with center frequencies ranging from 20 – 200 Hz in increments of 0.05 Hz.

The PV analysis highlights some potential issues in the phase response, even within the minimum phase range (shown in Fig. 3.3). The frequencies with high variance (such as 64, 82 and 128 Hz) are likely to exhibit poor transient responses. Of course, these variance peaks will broaden and decrease in amplitude for shorter tone-bursts (wider frequency analysis bands) and will tend to zero as pure-tone analysis is approached (since the variance between a single frequency bin has to be zero). This form of analysis is used in the following sections to help explain inconsistencies between magnitude and phase error.

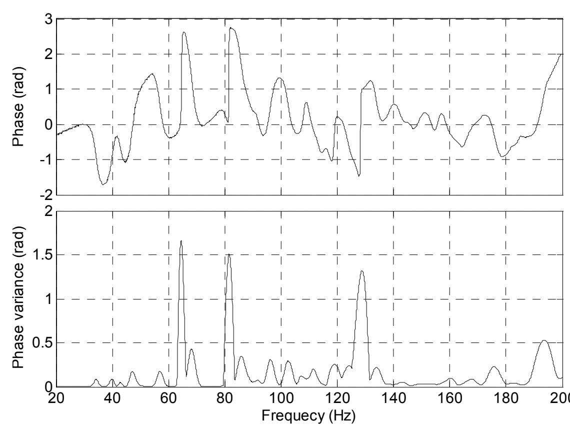

Fig. 3.4 Comparison of the ideal phase response (top) and its phase variance (bottom) for a 10-cycle tone burst

3.3. Experimental procedure

All measurements were taken in the University of Essex Audio Research Laboratory (ARL) listening room (dimensions 8.13 m x 6.14 m x 2.74 m). For consistency, simulations were conducted in a virtual space of similar dimensions and configuration (precisely equal dimensions aren't possible due to the finite spatial resolution of the FDTD procedure). Virtual and real-world MLS measurements were taken over a 16-point listening grid, spanning a 2.1 m x 2.1 m area with 70 cm spacing between points (Fig. 3.5). All measurements were taken at a height of 1.60 m.

Two subwoofer configurations were used for the simulated and practical measurements. The first consists of a single omnidirectional subwoofer in a room corner (7.53 m, 0.65 m). This configuration should excite all room-modes since source-to-room coupling is maximized at antinodal points, where a room corner holds antinodes for all modes [26].

The second configuration consists of two omnidirectional subwoofers placed on the floor at wall midpoints directly to the left and right of the listening area: (4.40 m, 0.65 m) and (4.17 m, 5.75 m). The subwoofers in this configuration lie near nodes for certain modes, causing minimal coupling and low modal excitation. Since only some room-modes are excited in this situation, magnitude error should be reduced from the corner placement scenario. Comparing the two situations offers clues as to how magnitude and phase error relate to one another with varying configurations.

The experimental configurations were tested in virtual space to give initial indications of magnitude and phase error correlation via the Hilbert transform. Magnitude deviation (MD) was calculated using Eq. 2.4 and phase variance (PV) was determined with Eq. 3.4.

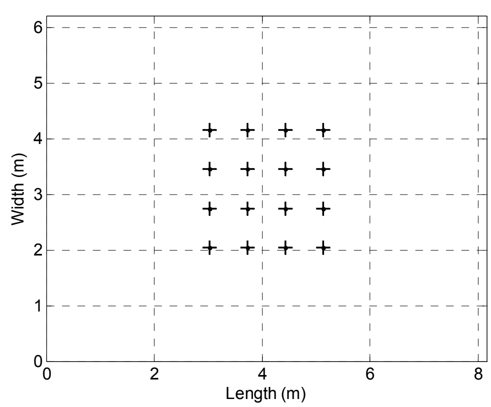

Fig. 3.5 Measurement point configuration in the University of Essex Audio Research Laboratory

The resulting data is spread over four dimensions: two spatial, one spectral and one magnitude (either MD or PV). This requires dimensional compression, of sorts, for clear data presentation. The data is therefore plotted two-dimensionally, whereby the horizontal x-axis represents the location index (progressing upwards through each column in Fig. 3.5, beginning with the left-most column and progressing to the right). Separating bars are included over the x-axis to delineate each column's measurement points. The vertical y-axis covers the frequency range of interest and the gray scale gives the MD or PV levels.

3.4. Simulation results – single subwoofer

One subwoofer in a room corner was modeled using an MLS excitation signal, where the impulse responses were extracted at sixteen measurement locations (see Fig. 3.5). MD and PV plots are given in Fig. 3.6. The two metrics were normalized to an absolute scale (0 – 1) to allow for a direct comparison.

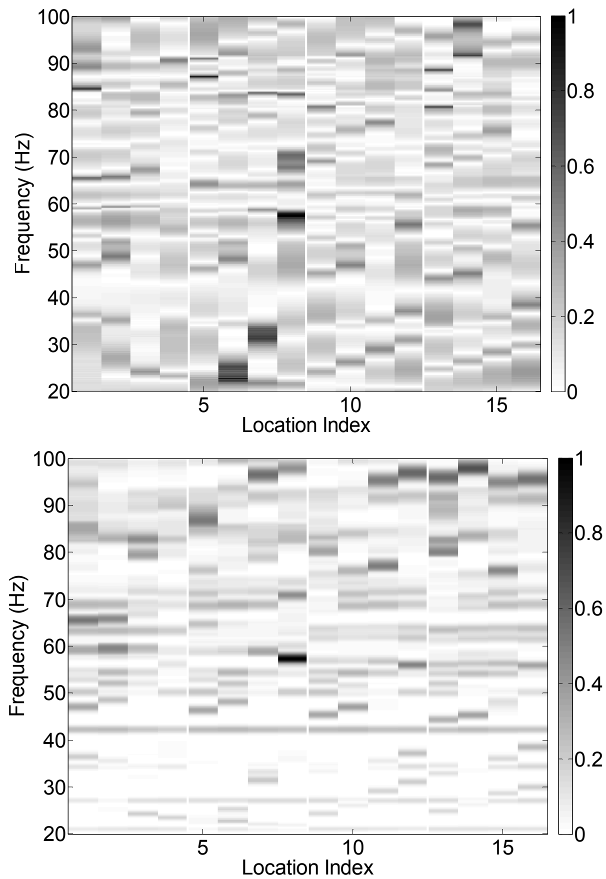

Fig. 3.6 Simulated MD (top) and PV (bottom) as a function of frequency and location index (see Fig. 3.5), as a result of a single corner subwoofer configuration

Upon first glance, the MD and PV plots seem to follow similar trends. For example, location 8 suffers from severe magnitude and phase error around 57 Hz, while locations 5 – 16 are relatively well-behaved in both domains around 65 Hz.

There are, however, a number of areas where magnitude and phase errors do not agree, such as at 42 Hz across all locations. In this case, magnitude error is minimal but phase error is moderate. These points may all exhibit similar steady-state responses, but will suffer from poor waveform fidelity due to PV.

As a detailed inspection may still pass over significant disagreements between magnitude and phase error, the differences between the two metrics at each measurement point are calculated in order to directly judge their level of agreement. Positive values indicate that the magnitude error outweighs the phase error, while negative values represent the contrary. An error agreement at or near zero points to strong magnitude and phase error agreement (Fig. 3.7).

Additionally, the data can be further compressed by finding the mean error agreement for each measurement point and then generating a spatio-distribution plot (Fig. 3.8) where the single corner subwoofer is located closest to point (4, 1). This allows for a more general inspection of the magnitude versus phase error over the listening area, considering the entire subwoofer band.

The error agreement plots show exactly how certain locations within a listening area can experience high magnitude error with minimal phase error, and vice versa. The lighter areas of Figs. 3.7 and 3.8 indicate poor waveform fidelity, but minimal magnitude error, while the darker areas signify the opposite.

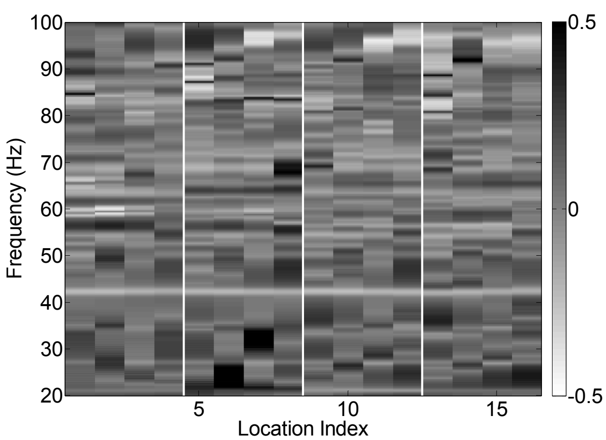

Fig. 3.7 Simulated error agreement as a function of frequency and location index (see Fig. 3.5), as a result of a single corner subwoofer configuration

Certain measurement points such as (1, 4), corresponding to location index 4 in Fig. 3.7, signify magnitude and phase error agreement. For this point, analyzing the magnitude error would give good indication of the phase error. However, critical to this study, this is not the case at every point in the listening area. Some points show very low error agreement, such as (3, 3), corresponding to location index 11 in Fig. 3.7, where little information concerning the phase error can be deduced from the magnitude error. The large negative value at (3, 3) indicates that there is minimal MD, but PV is moderate. The opposite can be said for (2, 4) where there is considerable magnitude error, but with high waveform fidelity.

It can be argued, therefore, that a low phase error with a high magnitude error is preferable to the contrary, provided the listener remains at their current location. Of course, in an optimum system both magnitude and phase errors would be minimized.

As both MD and PV were calculated based on components of a complex frequency response, it is important to check whether these metrics relate directly to the effects on actual program material. Upon inspection of the error agreement in Fig. 3.7, location index 8, or (2, 4) in Fig. 3.8, shows a dominant magnitude error. Location index 11, or (3, 3) in Fig. 3.8, indicates the opposite. An impulse response-derived 69 Hz tone burst (10 cycles per burst, 4 repetitions) was generated for points (2, 4) and (3, 3), which exhibit MDs of 12.7 dB and 4.4 dB and PVs of 0.09 and 0.49, respectively (Fig. 3.9).

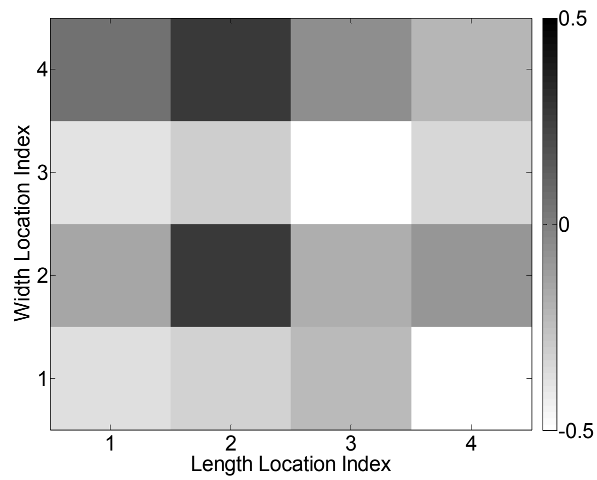

Fig. 3.8 Simulated mean error agreement as a function of location index (see Fig. 3.5) where point (1, 4) is closest to zero (perfect error agreement), as a result of a single corner subwoofer configuration

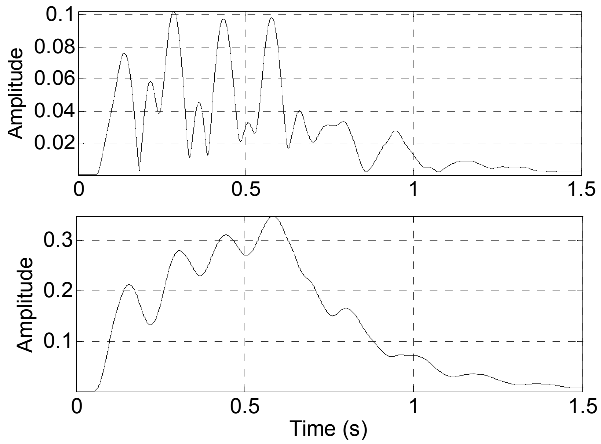

Fig. 3.9 69 Hz tone burst amplitude envelopes (10 cycles, 4 repetitions) at location index (1, 4) (top) and (3, 3) (bottom) relating to the data in Figs. 3.7 & 3.8

This example emphasizes precisely the cornerstone of this work: it is essential to analyze MD *and* PV to gather a complete understanding of the problem at hand. Even though magnitude and phase *responses* are directly related at this frequency (69 Hz), the magnitude and phase *errors* are quite different in nature and each must be addressed (the extent of waveform fidelity loss is not evident through direct inspection of the complex frequency response, although the extended analysis of the variance from an ideal phase response does highlight the problem very well).

3.5. Simulation results – multiple subwoofers

A two-subwoofer system utilizing sidewall midpoint placement effectively suppresses a number of problematic modes, thus providing a more consistent magnitude response across a wide-area [3,26]. This configuration was simulated as before, with error agreement plots in Figs. 3.10 and 3.11.

The dual-subwoofer system effectively suppresses the lower-order axial modes between 35 – 55 Hz, as evident with the slightly negative error agreement values in this range (indicating phase error outweighs magnitude error). Interestingly, the improvement in magnitude response does not translate to phase response improvements at many measurement points. In this case, the subwoofer configuration introduces waveform fidelity degradation, most notably around 32 and 42 Hz, likely due to arrival time differences between signals from the two subwoofers, but also as a result of the intersection of modal frequency bands at 35.0 Hz (tangential) and 42.3 Hz (axial), respectively.

While the measurement point columns exhibit response correlation due to the roughly symmetrical subwoofer layout (Fig. 3.11), there are few measurement points showing high error agreement (at least over the entire subwoofer band). As with the single subwoofer configuration, the dual wall midpoint configuration still gives poor error agreement over the listening area, highlighting the importance of examining magnitude and phase error when correcting for room-modes.

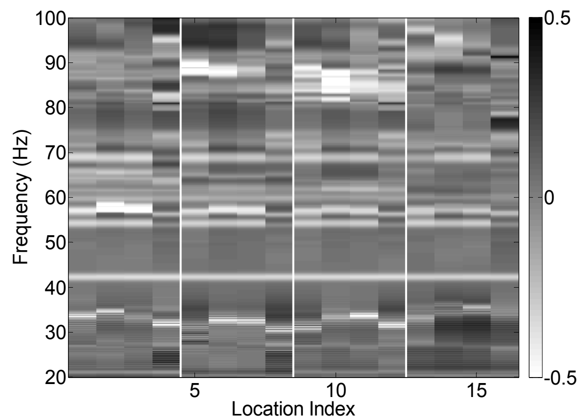

Fig. 3.10 Simulated error agreement as a function of frequency and location index (see Fig. 3.5), as a result of a two-subwoofer sidewall midpoint configuration

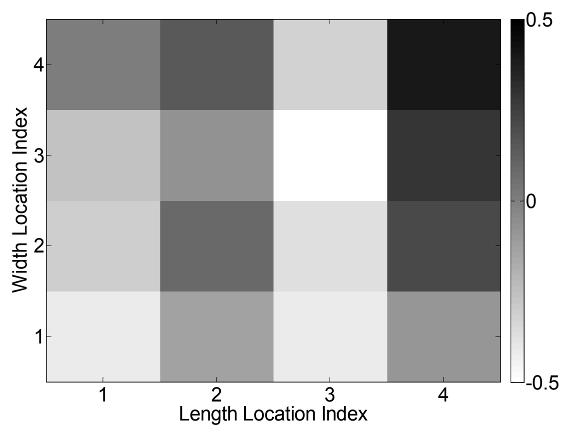

Fig. 3.11 Simulated mean error agreement as a function of location index (see Fig. 3.5) where point (1, 4) is closest to zero (perfect error agreement), as a result of a two-subwoofer sidewall midpoint configuration

3.6. Experimental results

While the simulation results offer strong evidence supporting close inspection of magnitude *and* phase error in small room acoustics, it is important to confirm these findings with practical measurements. The virtual experiments carried out in sections 3.3 and 3.4 were repeated, this time in the University of Essex Audio Research Laboratory listening room. The system configuration is identical to that described in section 3.2. While it is not expected that the experimental results will be perfectly in-line with the simulation results due to the many approximations in the virtual model (lack of room obstacles, finite grid spacing, resonant surfaces, non-ideal source characteristics, etc.), the underlying data trends should be in agreement.

The room corner and dual sidewall midpoint configuration results for the experimental trials are given in Figs. 3.12 and 3.13, respectively. Although the specific data distributions do not precisely agree with the simulation results, the general trends are consistent. The results support the overriding point that ideal system performance cannot be guaranteed solely with low magnitude error. This alone gives low spatial variance, but does not necessarily result in high waveform fidelity. This is precisely why phase response must be addressed within modal correction systems where tone bursts are suitable test signals to subjectively bring these issues to light.

3.7. Extended analysis - dipole sources

Dipole subwoofers are less common than omnidirectional sources, yet they have a strong following in the audiophile community which values them for their ability to maintain high waveform fidelity (low phase error) over a wide-area [25].

While omnidirectional units operate as pressure sources, dipoles behave as velocity sources. This means that modal coupling is minimized when dipoles are placed at sound pressure antinodes (particle velocity nodes). A common placement for dipole subwoofers is a quarter of the way along the room length on the sidewalls, which was simulated using two dipole sources to the left and right of the listening area (Fig. 3.14).

One interesting characteristic of the dipole system is that the error agreement is largely consistent (and near zero) over the listening area for frequencies below 55 Hz, where the only major issues occur at 42 Hz (due to a strong axial mode) and around 22 and 30 Hz (effects of comb filtering). The error agreement takes on a more randomized distribution above 55 Hz, as with the omnidirectional systems. In the lower region of the subwoofer band, however, there is evidence supporting the use of dipole subwoofers to suppress phase error over a wide listening area.

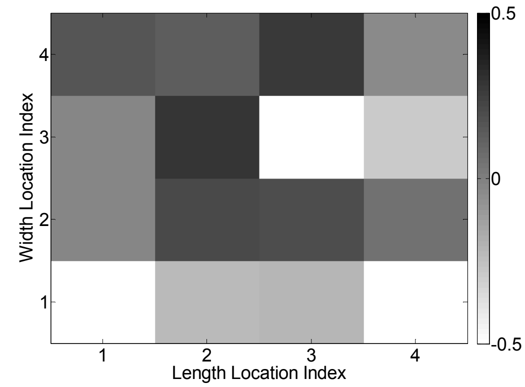

Fig. 3.12 Measured mean error agreement as a function of location index (see Fig. 3.5) where point (1, 3) is closest to zero (perfect error agreement), as a result of a single corner subwoofer configuration

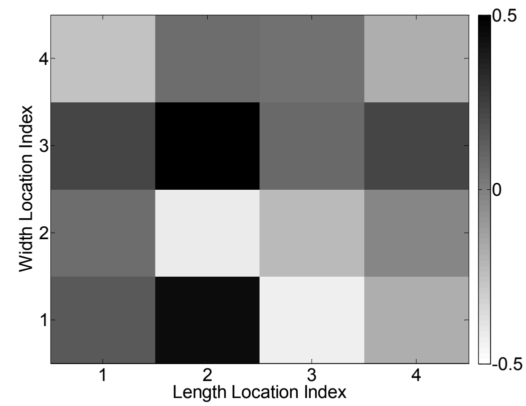

Fig. 3.13 Measured mean error agreement as a function of location index (see Fig. 3.5) where point (4, 2) is closest to zero (perfect error agreement), as a result of a two-subwoofer sidewall midpoint configuration

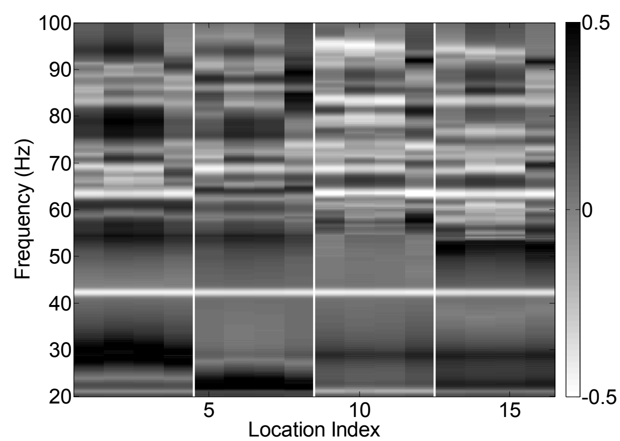

Fig. 3.14 Simulated error agreement as a function of frequency and location index, as a result of a two dipole subwoofer ¼ sidewall length configuration

3.8. Extended analysis – Single-point EQ

All analysis up to this point has concentrated on so-called "passive" correction or, in other words, systems that contain no specialized digital signal processing (DSP) geared towards modal correction. Although the passive correction methods indicate that magnitude and phase errors do not show strong correlation, it's possible the same cannot be said for "active" correction techniques (those which utilize DSP for correction).

As it has been shown in sections 3.1 and 3.2 that magnitude and phase errors are still related through the Hilbert transform (although the phase error calculation requires an additional layer of analysis), any active correction technique based on the complex frequency response should provide equal benefits to both domains.

One of the most common correction techniques is single-point equalization, whereby the frequency response is measured at a point in the listening area and an inverse filter is generated based on said measurement aiming for a "flat" response at that target point. This method was tested in the same virtual space as before, using the room corner subwoofer configuration. Measurement point (3, 3) from Fig. 3.8 was set as the target point as it exhibits high PV, but low MD.

This, therefore, will test if the single point equalization results in an improved transient response along with the desired flat magnitude response. Only the target point was analyzed in this case, as it is well known that a single point procedure only positively affects the target point, while other points generally suffer from degraded responses [10,14]. The unprocessed and processed magnitude and phase responses are directly compared in Fig. 3.15 with the PVs given in Fig. 3.16.

The single-point equalization procedure clearly serves to reduce both magnitude and phase error, therefore it is not necessary to worry about both domains; only tracking magnitude response improvements will suffice. The correction gives a very flat magnitude response and a phase response exhibiting considerably less PV than before (Fig. 3.16). The upward shift in the corrected phase response in Fig. 3.15 is due to a high-pass filter applied during correction to protect the subwoofer from over-excursion at very low-frequencies.

This serves as a good example of where phase error analysis is unnecessary. A minimum-phase equalization procedure such as this benefits magnitude and phase responses equally and therefore does not require any additional analysis.

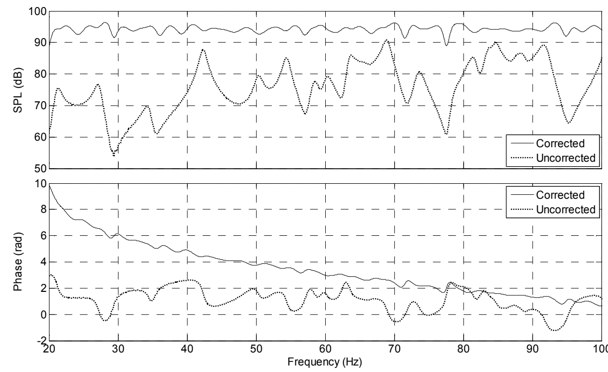

Fig. 3.15 Comparison of corrected and uncorrected magnitude (top) and phase (bottom) responses due to a single-point inverse-filter equalization procedure

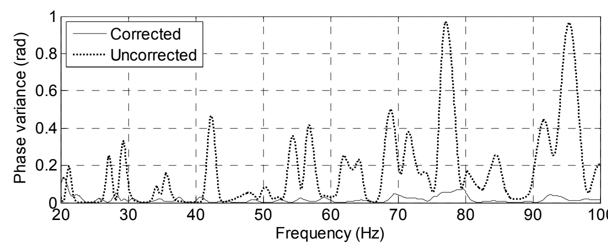

Fig. 3.16 Comparison of corrected and uncorrected PV due to a single-point inverse-filter equalization procedure

3.9. Extended analysis – Simple average EQ

The single-point equalization technique will only benefit the target point (at least in the low-frequency range). Following the theme of this paper, it is important to examine how a minimum-phase equalization procedure targeted over a number of measurement points behaves.

A very basic correction technique was tested which utilizes an inverse filter generated from the mean frequency response across a set of measurement points. While this technique won't give a flat frequency response, it should give similar changes in magnitude and phase error at each point, following the observations with the single-point technique.

The setup from section 3.8 was tested again with the corrected/uncorrected MD and PV values subtracted from one another to give a measure of how the correction has affected the response error. The change in error values are given for MD and PV in Figs. 3.17 and 3.18, respectively.

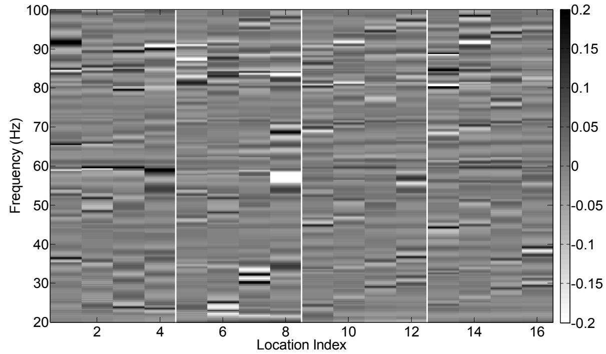

Fig. 3.17 Change in magnitude error due to simple average equalization (negative = improved response)

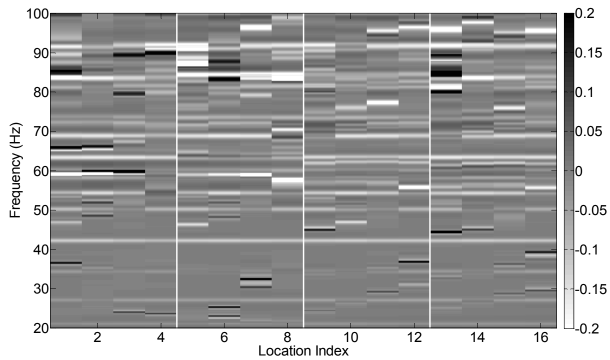

Fig. 3.18 Change in phase error due to simple average equalization (negative = improved response)

The changes in magnitude and phase error are largely in agreement after the simple average equalization. Most areas of disagreement can be attributed to the differing error metric calculation procedures. The only striking anomaly in this case is the improved phase response at 42 Hz with no change in the magnitude response. Interestingly, referring back to Fig. 3.6, there was a clear 42 Hz issue in the phase response, while no such issue existed in the magnitude response. Perhaps the correction procedure has somehow addressed this phase problem. This is an interesting occurrence, but it is designated as future work to find an explanation.

Nevertheless, as in the single-point procedure, the simple average correction does appear to benefit (or hurt) the magnitude and phase errors in a similar manner and, therefore, supports the conclusion from the previous section that it is only essential to inspect one domain when dealing with minimum-phase equalization methodologies.

4. PROPOSAL

The investigations into the relationship between magnitude and phase error in small-room low-frequency sound reproduction contained herein strongly underscore the necessity to analyze both domains when working with *passive* or *non-minimum-phase* correction techniques. Basing this sort of room-mode correction method solely on amplitude response *may* leave certain transient response errors unaddressed. This does not appear to be true for *minimum-phase* correction methods.

Concerning the magnitude domain, either spatial variance (Eq. 2.3) or MD (Eq. 2.4) can be used to quantify magnitude error over a listening area. Spatial variance (SV) is used more regularly, as it gives a single performance value for an entire space.

There does not exist a commonplace metric quantifying phase performance in relation to waveform fidelity. The authors therefore propose the use of phase variance (Eq. 3.4) to serve this purpose. Since phase variance (PV) addresses one measurement point at a time, mean PV can be determined in a similar manner to spatial variance (Eq. 4.1). PV in this case is calculated based on 10-cycle tone burst bandwidth, as this roughly corresponds to 1/3 octave spacing. The spatial variance calculation is reproduced here (Eq. 4.2) to make a complete set of equations for the proposal.

$$\overline{PV} = \frac{1}{N_f N_p} \sum_{i=1}^{N_f} \sum_{p=1}^{N_p} \sqrt{PV(p,i)} \tag{4.1}$$

$$SV = \frac{1}{N_f} \sum_{i=f_{lo}}^{f_{hi}} \sqrt{\frac{1}{N_p - 1} \sum_{p=1}^{N_p} \left(L_p(p,i) - \overline{L_p(i)}\right)^2} \tag{4.2}$$

where, $\overline{PV}$ is the mean phase variance, $PV(p,i)$ is the phase variance at the i^{th} frequency bin and the p^{th} measurement location, with N_f and N_p as the number of frequency bins and measurement locations, respectively. Note that SV is measured in decibels (logarithmic scale) while PV is in radians (linear scale).

Any effective room-mode correction system should therefore minimize *both* of these metric to ensure an improved listening experience over a wide-area. Failure to address PV will lead to problems highlighted in section 3 whereby magnitude response is minimized at the price of degraded waveform fidelity.

4.1. Subwoofer placement and polar pattern

A series of examples were tested in a 5 m x 4 m x 3 m virtual space (5% absorption on all surfaces) with a 25-point horizontal measurement grid centered at (3.0 m, 2.2 m, 1.8 m). SV and PV were calculated for the range spanning 20 – 100 Hz (Table 4.1).

Configuration	*SV (dB)*	*PV (rad)*
1 x room corner	6.023	0.272
1 x front wall midpoint	6.204	0.235
2 x front corners	6.082	0.255
2 x opposite corners	4.833	0.242
2 x side wall midpoints	3.639	0.196
4 x room corners	3.077	0.213
4 x wall midpoints	2.901	0.192
2 x dipoles, ¼ length	6.036	0.178

Table 4.1 Spatial variance and phase variance levels for eight simulated subwoofer configurations (sources are omnidirectional unless otherwise noted)

The SV and mean PV values relating to the various configurations highlight how magnitude and phase behavior do not always follow one another. Of all the systems tested, the two dipole subwoofers give the lowest phase error, which may explain audiophiles' devotion to dipoles. However, this system results in very high magnitude error. Of the omnidirectional subwoofer systems, those with multiple units placed at sidewall midpoints give the lowest phase error (aside from the dipoles) and relatively low magnitude error.

The underlying point here is that some system configurations benefit magnitude response more than phase response and vice versa. Only simple subwoofer placement adjustments were tested here, but the importance of including the two metrics for all passive room-mode correction methods should be clear.

5. CONCLUSIONS

The importance of considering phase alongside magnitude response is hinted at by Davis and Patronis [27]: "Measuring phase instead of magnitude provides greater sensitivity and resolution… phase response will typically be 10 times more sensitive than magnitude response." While this statement does not specifically point to magnitude versus phase *error*, it does highlight the importance of a correction system addressing both domains. Even if magnitude response is corrected properly, phase response (with its heightened sensitivity) is not guaranteed to benefit similarly when utilizing certain forms of correction such as multiple subwoofer placement or polar pattern adjustment.

There is not a complete disconnect between the two errors, however. A standard inspection of excess phase components (calculated directly from the impulse response) indicates that there is minimum phase behavior throughout the subwoofer band (~20 – 100 Hz in this scenario). While this does not indicate any phase issues, there are indeed problems which are highlighted using tone burst analysis. There must be a link, then.

This research pointed to phase response deviation from an ideal response as the "missing link." As Linkwitz (and others) have suggested, tone bursts allow for objective and subjective testing simultaneously since the signals relate well to standard program material. Keeping this in mind, it was found that tracking phase variation over the bandwidth of a tone burst flags frequency bands with high phase error. These results line up well with mean absolute error measurements gathered from tone burst testing, indicating the proposed link is likely genuine.

With this new information in mind, the authors propose that passive (or non-minimum phase) room-mode correction systems should continue to target spatial variance minimization, but additionally focus on phase variation minimization. Achieving low values for both will ensure desirable magnitude and phase responses across a wide-area. This is not necessary for minimum phase correction techniques.

In cases where simultaneous metric minimization is not possible, it is best to focus on phase error (assuming listeners aren't moving about) since high waveform fidelity is subjectively more desirable than magnitude response homogeneity between listeners. This is in line with audiophiles' preference for dipole subwoofers. The dipole units (as shown in this research) do little to suppress magnitude error, but generate minimal phase error providing high waveform fidelity.

While the authors are not suggesting researchers start from scratch with room-mode correction (there are indeed many excellent correction methods out there), they do suggest that correction techniques be examined for phase error and adjusted accordingly. Targeting both forms of error will give conclusive proof that a system has acceptable objective performance. Subjective performance is a different story, of course.

6. REFERENCES

[1] Walker, R. "Optimum dimension ratios for small rooms." 100th AES Convention, paper 4191. May, 2002.

[2] Milner, J.R; R.J. Bernhard. "An investigation of the modal characteristics of nonrectangular reverberation rooms." JASA, vol. 85, no. 2, pp. 772-779. February, 1989.

[3] Welti, T.; A. Devantier. "Low-frequency optimization using multiple subwoofers." Journal of the Audio Engineering Society, vol. 54, no. 5, pp. 347-364. May, 2006.

[4] Celestinos, A.; S. Birkedal Nielsen. "Multi-source low frequency room simulation using finite different time domain approximations." 117th AES Convention, paper 6264. October, 2004.

[5] Reiley, E.; A. Grimani. "Room mode bass absorption through combined diaphragmatic & Helmholtz resonance techniques: 'The Springzorber.'" 114th AES Convention, paper 5760. March, 2003.

[6] Vanderkooy, J. "Multi-source room equalization: Reducing room resonances." 123rd AES Convention, paper 7262.October, 2007.

[7] Makivirta, A.; P. Antsalo; M. Karjalainen; V. Valimaki. "Modal equalization of loudspeaker room responses at low frequencies." JAES, vol. 51, no. 5, pp. 324-434. May, 2003.

[8] Genereux, R.P. "Adaptive loudspeaker systems: correcting for the acoustics environment." 8th International Conference of the AES. May, 1990.

[9] Kuriyama, J.; Y. Furukawa. "Adaptive loudspeaker system." JAES, vol. 37, no. 11, pp. 919-926. November, 1989.

[10] Elliot, S.J.; L.P. Bhatia; D.W. Deghan; A.H. Fu; M.S. Stewart; D.W. Wilson. "Practical implementation of low-frequency equalization using adaptive digital filters." JAES, vol. 42, no. 12, pp. 988-998. December, 1994.

[11] Santillan, A.O. "Spatially extended sound equalization in rectangular rooms." JASA, vol. 110, no. 4, pp. 1989-1997. October, 2001.

[12] Bharitkar, S.; C. Kyriakakis. "Objective function and automatic multi-position equalization and bass management filter selection." 119th AES Convention, paper 6608. October, 2005.

[13] Backman, J. "Low-frequency polar pattern control for improved in-room response." 115th AES Convention, paper 5867. October, 2003.

[14] Hill, A.J. "Analysis, modeling and wide-area spatiotemporal control of low-frequency sound reproduction." Ph.D. Thesis, University of Essex, UK. January, 2012.

[15] Pedersen, J.A. "Adjusting a loudspeaker to its acoustic environment – The ABS system." 115th AES Convention, paper 5880. October, 2003.

[16] Howe, R.M.; M.O.J. Hawksford. "Methods of local room equalization and their effect over the listening area." 91st AES Convention, paper 3138. October, 1991.

[17] Hayes, M.H.; J.S. Lim; A.V. Oppenheim. "Signal reconstruction from phase or magnitude." IEEE Transactions on Acoustics, Speech, and Signal Processing, vol. 28, no. 6, pp. 672-680. December, 1980.

[18] Kuttruff, H. "Sound fields in small rooms." 15th International AES Conference, paper 15-002. October, 1998.

[19] M.R. Schroeder. "Statistical parameters of the frequency response curves of large rooms." JAES, vol. 35, no. 5, pp. 299-306. May, 1987.

[20] Kemp, J.A. "Improvements to bore profile measurement in acoustic pulse reflectometry." Proc. Institute of Acoustics, vol. 30, pt. 2. 2008.

[21] Corrington, M.S. "Correlation of transient measurements on loudspeakers with listening tests." JAES, vol. 3, no. 1, pp. 35-39. January, 1955.

[22] Kaminsky, V.J. "The response of loudspeaker to tone bursts." JAES, vol. 13, no. 2, pp. 119-123. April, 1965.

[23] Linkwitz, S. "Narrow band impulse testing of acoustical systems." 60th AES Convention, paper 1342. May, 1978.

[24] Linkwitz, S. "Shaped tone-burst testing." JAES, vol. 28, no. 4, pp. 250-258. April, 1980.

[25] Linkwitz, S. "Investigation of sound quality differences between monopolar and dipolar woofers in small rooms." 105th AES Convention, paper 4786. September, 1998.

[26] Toole, F.E. *Sound Reproduction: Loudspeakers and Rooms*. Focal Press, Boston, MA. 2008.

[27] Davis, D.; E. Patronis Jr. *Sound System Engineering: Third Edition.* Focal Press, Boston, MA. 2006. p. 139.